THERMODYNAMICS OF CARBON REMOVAL BY MOLTEN SLAGS FROM MANGANESE ALLOY MELTS

J.H. Park[1], G.H. Park[1], C.I. Park[1], J.G. Park[2], D.J. Min[2], H.C. Jo[3], and Y.E. Lee[3]

[1] School of Materials Science and Engineering, University of Ulsan, Ulsan, Korea;
basicity@mail.ulsan.ac.kr (contact author; JHP)
[2] Department of Materials Science and Engineering, Yonsei University, Seoul, Korea;
chemical@yonsei.ac.kr
[3] Metallic Materials Research Institute, Dongbu Metal Co. Ltd., Donghae, Korea;
hccho@dongbu.com, young.lee@dongbu.com

ABSTRACT

The carbon refining ability of the CaO-SiO_2-MnO slag was measured at 1773 K by employing a carbide capacity concept. Also, in-situ dissolution behaviour of SiC particle into the slag was directly observed by using a confocal scanning laser microscope (CSLM) at 1873 K. The carbide capacity was confirmed to be strongly dependent on the basicity and the stability of carbide ions. The carbide capacity also increased with increasing optical basicity of the slag, indicating that the optical basicity can be applied as a measuring index for the carbide capacity of MnO-containing slags. In the CSLM experiments, the SiC particles continuously dissolved into the slag through the wetting phenomena by molten slag and followed by the evolution of gas bubbles. The more basic slags enhanced the wetting of SiC particle by the slag. The fine bubbles were probably believed to be Mn(g) and CO(g) produced from the reaction between SiC particle and MnO in the slag. The more basic slag also seems to increase the apparent dissolution rate of SiC particles due to lower viscosity.

1 INTRODUCTION

A flexible electric furnace operation has widely been used in production of manganese ferroalloys such as high carbon ferromanganese (HC FeMn) and silicomanganese (SiMn), according to requirement. There are two operational strategies referred to as the discard slag practice (or basic slag operation) and the high MnO practice (or fluxless operation) [1]. In the latter, the MnO-rich slag is reprocessed for production of SiMn in duplex processing. In this way, the MnO content of the discard slag can be reduced to 5 to 10 mass% MnO. There has been a shift in demand in many countries away from the use of HC FeMn towards SiMn and refined alloys of both.

Low carbon SiMn with 20~30 mass% Si is produced by upgrading standard SiMn alloy by the addition of Si wastes from ferrosilicon industry. The Mn(-Fe)-Si-C system is an important metallic system in production of SiMn [1]. Graphite is the stable phase in the lower Si range. When the Si content is raised to a certain value at a fixed temperature, the coexistence point is reached where the liquid alloy will be in equilibrium with both graphite and silicon carbide (SiC). At Si-contents above this point, SiC will become the stable phase. Therefore, the addition of Si decreases the solubility limit of carbon in SiMn alloy melt. Notwithstanding this well-known thermodynamic information, there are few experimental data for understanding the refining mechanism of carbon (or SiC) from SiMn melt.

Based on the above backgrounds, in the present study, the carbon refining ability of the CaO-SiO_2-MnO slag system was measured at 1773 K by employing a carbide capacity concept and thermochemical equilibration methodology. Furthermore, *in-situ* dissolution behaviour of SiC particle into the slag was directly observed by using a confocal scanning laser microscope (CSLM) at 1873 K.

2 THEORETICAL CONSIDERATION

Since the late 1960's, carbon has been known to dissolve into the slags as a free carbide (C_2^{2-}) and a carbonate (CO_3^{2-}) in the reducing ($p_{O_2} < 10^{-15} atm$) and oxidizing ($p_{O_2} > 10^{-10} atm$) atmosphere,

respectively [2-12]. Thus, it can be confirmed that the stable ionic form is carbide under reducing atmosphere, which is in correspondence to the manganese alloy production. The solubility of carbon generally increased with increasing basicity in the lime-based silicate, aluminate, and aluminosilicate slags with and without fluorspar, whilst it increased by increasing the content of silica in the aluminosilicate slags at a fixed lime to alumina ratio [2,5]. The only slag system containing manganese oxide in view of carbon dissolution behaviour was the BaO-MnO flux, where the carbon solubility increased by increasing BaO content not only due to a basic characteristic of BaO but also due to a strong ionic attraction between Ba^{2+} cation and carbide anion [12].

The solubility of carbon in metallurgical slags has been quantitatively investigated by employing the carbide capacity concept (Eq. (2)) defined from a dissolution reaction which is given in Eq. (1) [3-11].

$$2C(s) + O^{2-}(slag) = C_2^{2-}(slag) + \frac{1}{2}O_2(g) \quad (1)$$

$$C_{C_2^{2-}} \equiv \frac{K_{(1)} \cdot a_{O^{2-}}}{f_{C_2^{2-}}} = \frac{(mass\%C_2^{2-}) \cdot p_{O_2}^{1/2}}{a_C^2} \quad (2)$$

where: $K_{(1)}$ = equilibrium constant of Eq. (1);

$a_{O^{2-}}$ = activity of O^{2-} ion in slag (= basicity of slag);

$f_{C_2^{2-}}$ = activity coefficient of carbide (C_2^{2-}) ion in slag;

p_{O_2} = oxygen partial pressure.

In case of carbon saturation condition, the activity of carbon is unity. Hence, the carbide capacity can be estimated from the product between the solubility of carbon and the square root of oxygen partial pressure. From a definition of carbide capacity (Eq. (2)), it is a function of basicity and the stability of carbide ions in molten slags at a fixed temperature.

The stability of carbide ions in the slags can be estimated from the Gibbs free energy of the formation of CaC_2 (Eq. (3)) [13,14], which is the most stable species in the present conditions. That is, the formation of CaC_2 is thermodynamically more pronounced reaction than that of SiC and Mn_3C.

$$CaO(s) + 2C(s) = CaC_2(s) + \frac{1}{2}O_2(g), \ \Delta G^{o} = 568000 - 144T \text{ (J/mol)} \quad (3)$$

$$K_{(3)} = \frac{\gamma_{CaC_2} \cdot X_{CaC_2} \cdot p_{O_2}^{1/2}}{a_{CaO} \cdot a_C^2} \quad (4)$$

$$\log \gamma_{CaC_2} = \log a_{CaO} - \log X_{CaC_2} - \frac{1}{2}\log p_{O_2} + \log K_{(3)} \quad (5)$$

where: γ_{CaC_2} = activity coefficient of CaC_2 in the slag.

The calculated values of the activity of CaC_2 in the present experimental conditions are less than about 10^{-4}. Therefore, the discussion in the present study will be limited to the dissolved carbide ions in molten slags. In this study, the activity of slag components in the CaO-SiO_2-MnO system was calculated by using commercial thermochemical computing software, FactSage6.1™ using *FToxid* database [15]. In this database, the systems containing MnO with major oxide components such as CaO and SiO_2, that is CaO-MnO, MnO-SiO_2, and CaO-MnO-SiO_2, are fully evaluated and optimized based on the Gibbs free energy minimization principle [16].

3 EXPERIMENTAL PROCEDURE

3.1 Measurement of Carbide Capacity

A super-kanthal electric resistance furnace was used for an equilibration of the CaO-SiO_2-MnO slag and gas phase at 1773 K. The temperature was controlled within ±2 K using an R-type (Pt-13%Rh/Pt)

thermocouple and a proportional integral differential controller. The furnace temperature was also calibrated using a B-type (Pt-30%Rh/Pt-6%Rh) thermocouple. The slag samples were prepared using reagent-grade SiO_2, MnO and CaO calcined from $CaCO_3$. For the saturation conditions with silica and dicalcium silicate phase, a piece of pure quartz and lime crystals (> 99.9 mass%) are located in the slag. A schematic diagram of the experimental apparatus is shown in Figure 1.

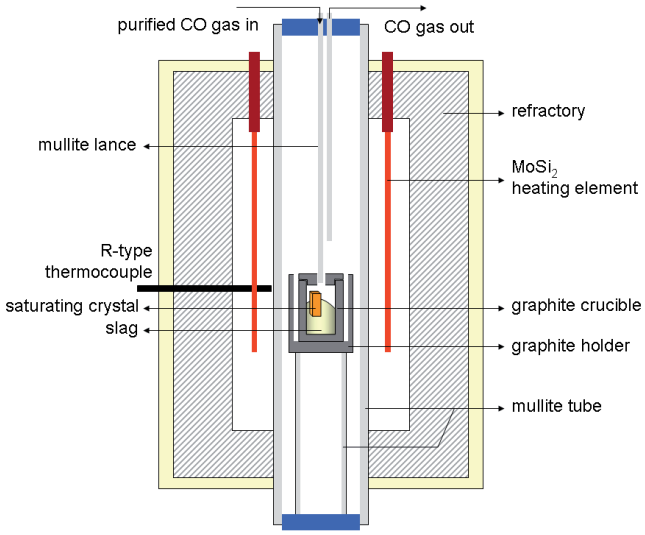

Figure 1: Schematic diagram of the experimental apparatus for measuring the carbide capacity.

The slag sample of 4 g was maintained in a graphite crucible under CO atmosphere (200 ml/min) to control the oxygen partial pressure by C/CO equilibrium reaction, as given in Eq. (6) [17].

$$C(s) + \frac{1}{2}O_2(g) = CO(g), \quad \Delta G^{o} = -114000 - 85.8T \text{ (J/mol)} \tag{6}$$

The impurities such as CO_2 and H_2O in the CO gas were removed by passing through silica gel, drierite®, magnesium perchlorate, and soda lime. The equilibration time was predetermined to be 15 hours. After equilibrating, the sample was quickly drawn from the furnace and quenched by Ar flushing and water. The quenched samples were crushed to less than 100 μm using stainless and agate mortar for chemical analysis. The content of total carbon and each component in the slags were determined by a combustion analyzer (LECO, CS-200) and X-ray fluorescence spectroscopy (Bruker, S4 Explorer). The equilibrium compositions of the slag investigated in this study are shown in Figure 2.

3.2 In-situ Observation of Dissolution Behaviour of SiC Particle

A confocal scanning laser microscope (CSLM) with a high temperature cell (Lasertec, VL2000DX) was used. In the CSLM, high-resolution images of material can be obtained that cannot be produced by most other conventional imaging techniques. Such imaging enables real time *in-situ* observation of high-temperature (~1873 K) transient phenomena. Also, the advantage of the CSLM technique with reference to traditional dissolution experiments using rods and cylinders is that the ratio of the volume of dissolving species to the volume of the solvent slag is very small [18]. Therefore, dissolution takes place without significant changes in the bulk composition of the slag.

The compositions of the slags used in this study are CaO-SiO_2-10 mass% MnO (lime/silica = C/S = 1.0) and CaO-SiO_2-20 mass% MnO (C/S = 0.5). These systems are important in production of manganese alloys even though small amounts of Al_2O_3 and MgO are not included for the sake of simplification [1]. The slags were prepared by mixing the reagent-grade oxides and melting the mixture in a platinum crucible in a tube furnace under Ar at 1773 K. After melting, the slag was quenched against a steel plate. A piece of quenched slag (~0.15 g) was then melted again in the CSLM before running an experiment. During an experiment, it is possible to follow the trajectory of the particle and keep focusing on it on the surface of the liquid slag.

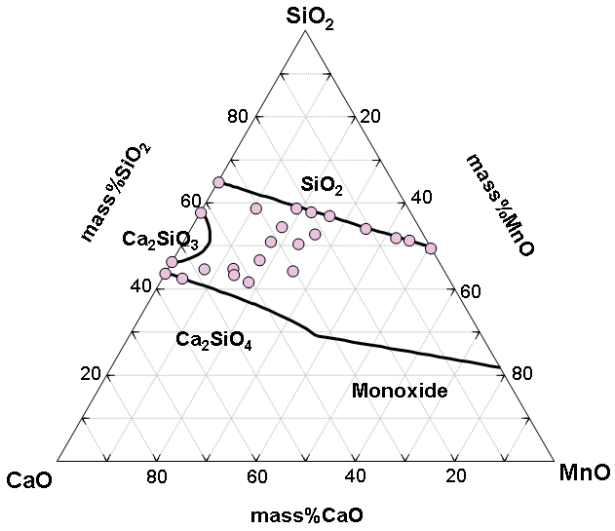

Figure 2: Phase diagram of the CaO-SiO_2-MnO slag at 1773 K and the experimental compositions.

The dissolution studies took place in a platinum crucible (4 mm in inner diameter and a height of 5 mm) by placing a piece of SiC (> 99.9 mass%) particle on the surface of a solid slag and heating this assembly to 1873 K under an ultrahigh-purity flowing Ar atmosphere (200 ml/min). The Ar atmosphere was repeatedly switched to vacuum three times. Figure 3 shows the schematic representation of (a) a halogen lamp chamber, (b) a sample holder assembly and (c) temperature profile used in the experiments. The video recordings of the dissolution process were analyzed to obtain the change in particle size with time. Because the shape of the initial SiC particle was not spherical but plate-like, the largest diagonal distance of the particle was represented in this paper. The quenched sample was also observed by using SEM-EDS.

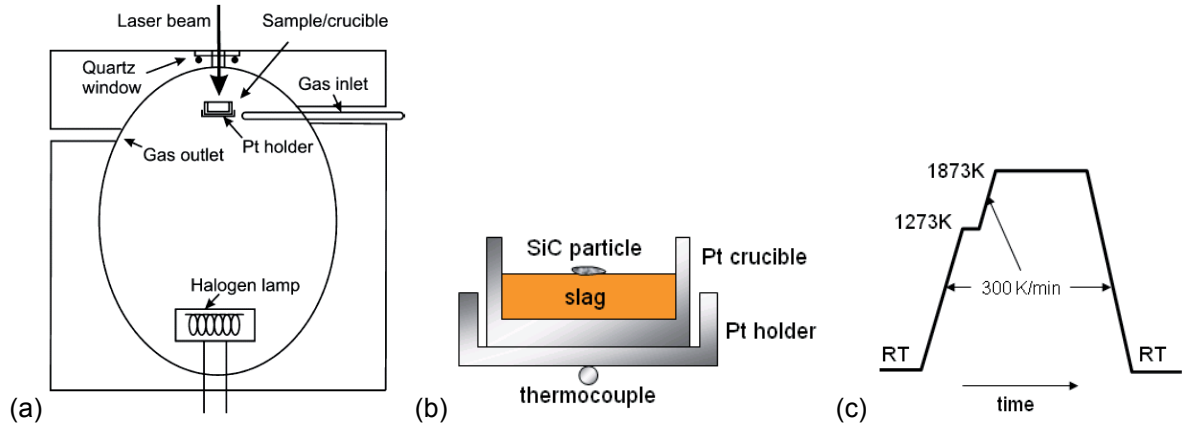

Figure 3: Schematic representation of (a) a halogen lamp chamber of CSLM, (b) a sample holder assembly and (c) temperature profile used in the experiments.

4 RESULTS AND DISCUSSION

4.1 Effect of Slag Composition on Carbide Capacity of CaO-SiO_2-MnO Slag

The carbide capacity of the silica saturated system is shown in Figure 4 as a function of MnO content at 1773 K. The carbide capacity decreases with increasing concentration of MnO to about 30 mass%, followed by a nearly constant value at MnO > 30 mass%. This tendency of carbide capacity can be

understood by that of basicity and stability of carbide ions in this system. Because the activity of free O^{2-} ions cannot be measured due to a thermodynamic constraint, the activity of lime is assumed to be directly proportional to that of O^{2-} ions based on the following dissociation equilibrium [7-11].

$$(CaO) = (Ca^{2+}) + (O^{2-}) \quad (7)$$

$$\log a_{CaO} = \log a_{O^{2-}} + \log a_{Ca^{2+}} - \log K_{(7)} \quad (8)$$

The stability of carbide ions can be estimated by employing the activity coefficient of CaC_2 as discussed in Section 2. Figure 5 shows the value of $\log a_{CaO}$ and $\log \gamma_{CaC_2}$ as a function of MnO content in silica saturated slag system at 1773 K. The $\log \gamma_{CaC_2}$ does not change to about 30 mass% MnO and then decreases, whilst the $\log a_{CaO}$ continuously decreases with increasing content of MnO. In this system, as shown in Figure 2, the content of CaO drastically decreases with increasing MnO content for maintaining silica saturation condition. Hence, the activity of lime linearly decreases through the wide range of composition, resulting in the initial decrease and final level-off of the carbide capacity based on its definition (Eq. (2)). This indicates that the manganese oxide could stabilize the carbide ions in the manganese silicate system.

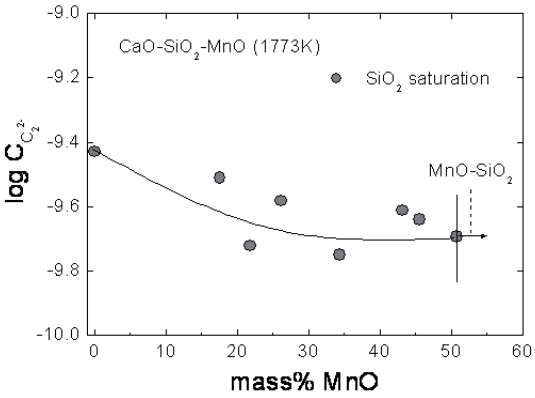

Figure 4: Effect of MnO content on carbide capacity of silica saturated system.

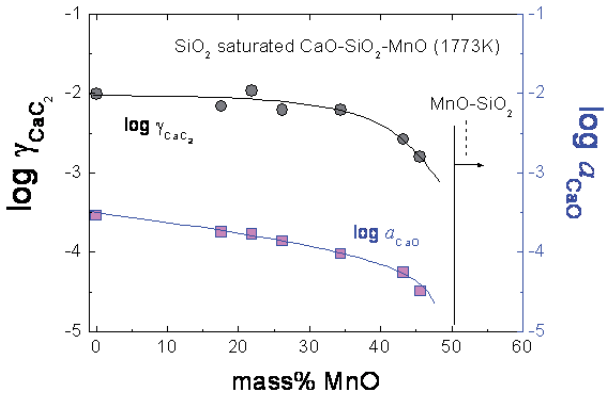

Figure 5: Activity of lime and activity coefficient of carbide in the silica saturated slag.

The effect of lime content on the carbide capacity of the CaO-SiO_2-MnO (MnO/SiO_2 = 0.3~0.4) system at 1773 K is shown in Figure 6. The carbide capacity exhibits a maximum value at 35 mass% CaO under fixed MnO/SiO_2 ratio. In this composition range, as shown in Figure 7, the activity of lime linearly increases by increasing its content, whilst the activity coefficient of carbide does not change till 35 mass% CaO, followed by an abrupt increase at CaO > 35 mass%.

The relationship between the carbide capacity and the ratio of lime to silica (C/S) at 1773 K is shown in Figure 8. In the CaO-SiO_2 binary system, the carbide capacity sharply increases at C/S > 1.0, which is mainly due to a stabilization of carbide ion by Ca^{2+} cation in the basic composition such as dicalcium silicate saturated system as shown in Figure 9. In MnO-containing ternary slag, the carbide capacity shows a maximum value at C/S = 0.8. In ternary system containing MnO from 15 to 25 mass%, the activity of lime continuously increases with increasing C/S ratio, whereas the activity coefficient of carbide abruptly increases at C/S > 0.8 as shown in Figure 9. Consequently, the manganese oxide about 15~25 mass% partly contributes to an increase in the carbide capacity at C/S = 0.6~1.0, whereas it decreases the carbide capacity in the acidic compositions, *viz*. C/S < 0.6.

The carbide capacity of the MnO-containing slags is plotted against the activity of lime in Figure 10. The effect of lime activity on the carbide capacity is negligible in the silica saturated system. However, the carbide capacity linearly increases with increasing activity of lime in logarithmic scale with the slope of about 0.75, which is slightly less than theoretically expected value of unity in Eqs. (2) and (8) in the liquid slag. Therefore, it is suggested that an increasing rate of $a_{Ca^{2+}}$ is greater than a

decreasing rate of $f_{C_2^{2-}}$ as the activity of lime increases, which is probably due to a complex effect of Ca^{2+} and Mn^{2+} on the stability of carbide ions.

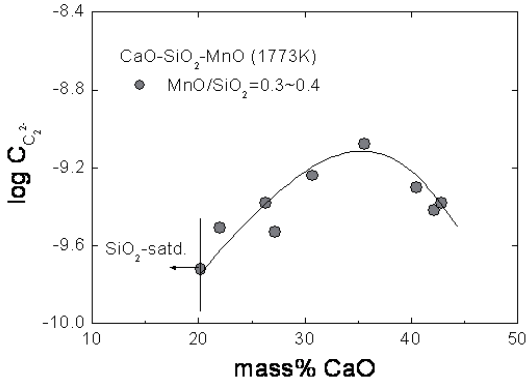

Figure 6: Effect of CaO content on carbide capacity at a fixed MnO/SiO_2 ratio.

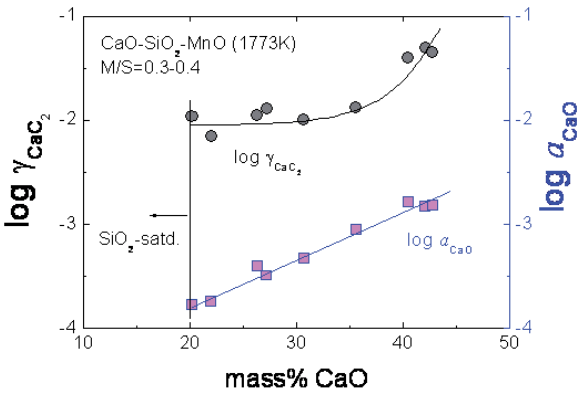

Figure 7: Activity of lime and activity coefficient of carbide at a fixed MnO/SiO_2 ratio.

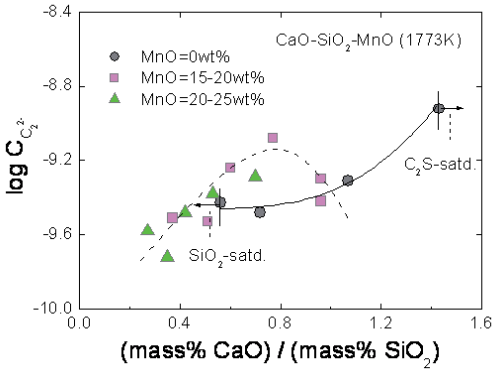

Figure 8: Effect of C/S ratio on the carbide capacity at a fixed MnO content.

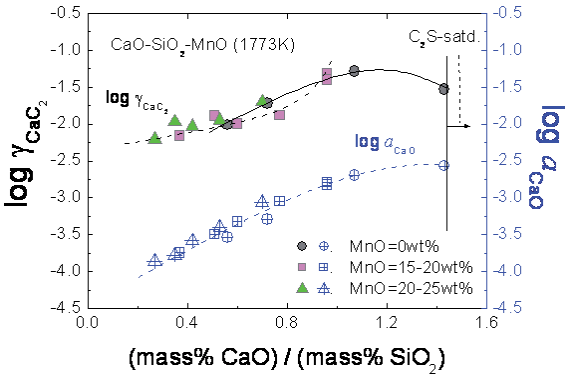

Figure 9: Activity of lime and activity coefficient of carbide at a fixed MnO content.

The effect of slag composition on the carbide capacity can be expressed by employing a theoretical optical basicity as an indirect basicity index. Figure 11 shows a relationship between carbide capacity and theoretical optical basicity of the $CaO-SiO_2-MnO$ slag at 1773 K. Here, the optical basicity of molten slags (Λ_{melt}) can be calculated from Eq. (9) [7,11,19].

$$\Lambda_{melt} = \frac{\sum x_i n_i \Lambda_i}{\sum x_i n_i} \tag{9}$$

where: x_i = mole fraction of oxide

n_i = number of oxygen in each oxide

Λ_i = theoretical optical basicity of each oxide *i*, *i.e.* $\Lambda_{CaO} = 1.0$, $\Lambda_{MnO} = 1.0$, $\Lambda_{SiO_2} = 0.48$.

Even though Sosinsky and Sommerville proposed $\Lambda_{MnO} = 1.2$ for the estimation of sulphide capacity of the metallurgical slags [20], the original value ($\Lambda_{MnO} = 1.0$) suggested by Duffy was employed in the present study [19]. The carbide capacity linearly increases with increasing optical basicity with some scatters. The 95% confidence limit is also shown. It is interesting that the present results are

relatively close to the relationship between carbide capacity and optical basicity in the lime-based silicate and aluminate slags containing fluorspar [9,11]. Thus, the optical basicity is one of the methods to estimate the carbide capacity of the MnO-containing slags through the wide composition range.

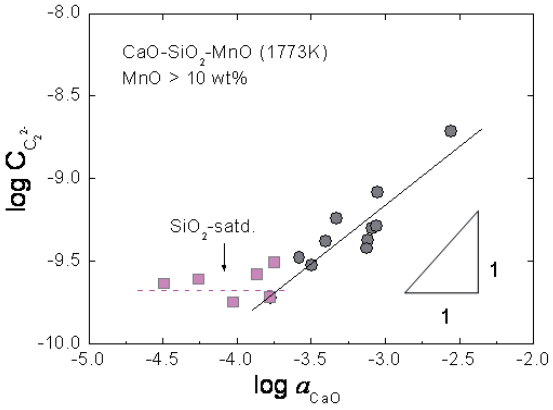

Figure 10: Relation between carbide capacity and lime activity in the slag.

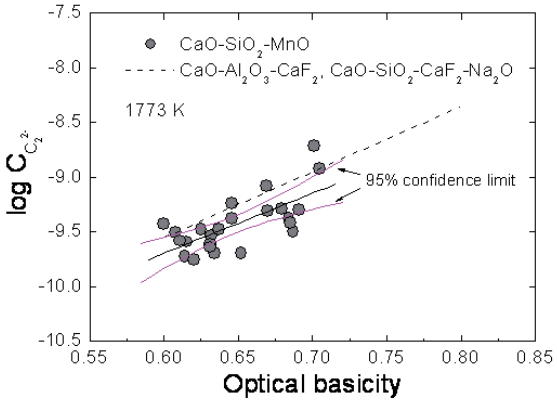

Figure 11: Relationship between carbide capacity and optical basicity of the slag.

4.2 In-situ Observation of Dissolution Behaviour of SiC Particle into CaO-SiO_2-MnO Slag

In the SiMn refining process by adding Si sources, the SiC forms at silicon content greater than about 22 mass% when the carbon content would be 1.0 mass% at 1773 K [1]. Thus, SiC particles could be nucleated and grown in the melt, followed by floatation to the slag/metal interface. However, there is few reports on the observation of the dissolution phenomena of SiC particle into the slags at high temperatures. Therefore, in this study, the dissolution behaviour of SiC particle is directly observed by using CSLM as described in Section 3.2.

The variations of morphology and size of SiC particles with reaction time are shown in Figure 12 (a) for the 45 mass% CaO-45 mass% SiO_2-10 mass% MnO system (slag A) and (b) for the 27 mass% CaO-53 mass% SiO_2-20 mass% MnO system (slag B) at 1873 K. The SiC particles gradually shrink as the reaction time increases through the wetting by molten slags from the outer surface. As shown in Figure 12 (a), the wetting tendency by molten slag was more pronounced in case of the more basic system (slag A), where the outer surface of SiC particle was wetted by molten slag at very early stage and fully wetted by the slags at about 12 min. at 1873 K. However, the SiC particle was wetted by the relatively acidic (C/S = 0.5) system (slag B) at about 6 min. later at 1873 K but not fully wetted by the slag through the entire holding time, *i.e*. 30 min. in the present experiment as shown in Figure 12 (b).

This is very interesting result, which can be explained by the recent work by Safarian and Tangstad [21]. They measured the wettability of SiC substrate by liquid CaO-SiO_2 slags (C/S = 0.7~1.1) using a sessile drop technique and found that the wettability was relatively high for the basic slag. Even though the effect of MnO on the wettability between SiC and molten slag was not taken into account in their study, the present *in-situ* observation results using CSLM shown in Figure 12 are in good correspondence to the results measured by Safarian and Tangstad.

Furthermore, when the SiC particle dissolved into the slags, bubble bursting phenomena at the SiC/slag interface as well as at the wetted surface of SiC particle was also observed. This bubble could be composed by gaseous manganese and carbon monoxide based on Eq. (10) [17].

$$3MnO(s) + SiC(s) = SiO_2(s) + 3Mn(g) + CO(g),\ \Delta G^o = 963120 - 474T\ (J/mol) \quad (10)$$

$$p_{Mn}^3 \cdot p_{CO} = K_{(10)} \cdot \frac{a_{MnO}^3}{a_{SiO_2}} \quad (11)$$

where the activity of SiC is unity.

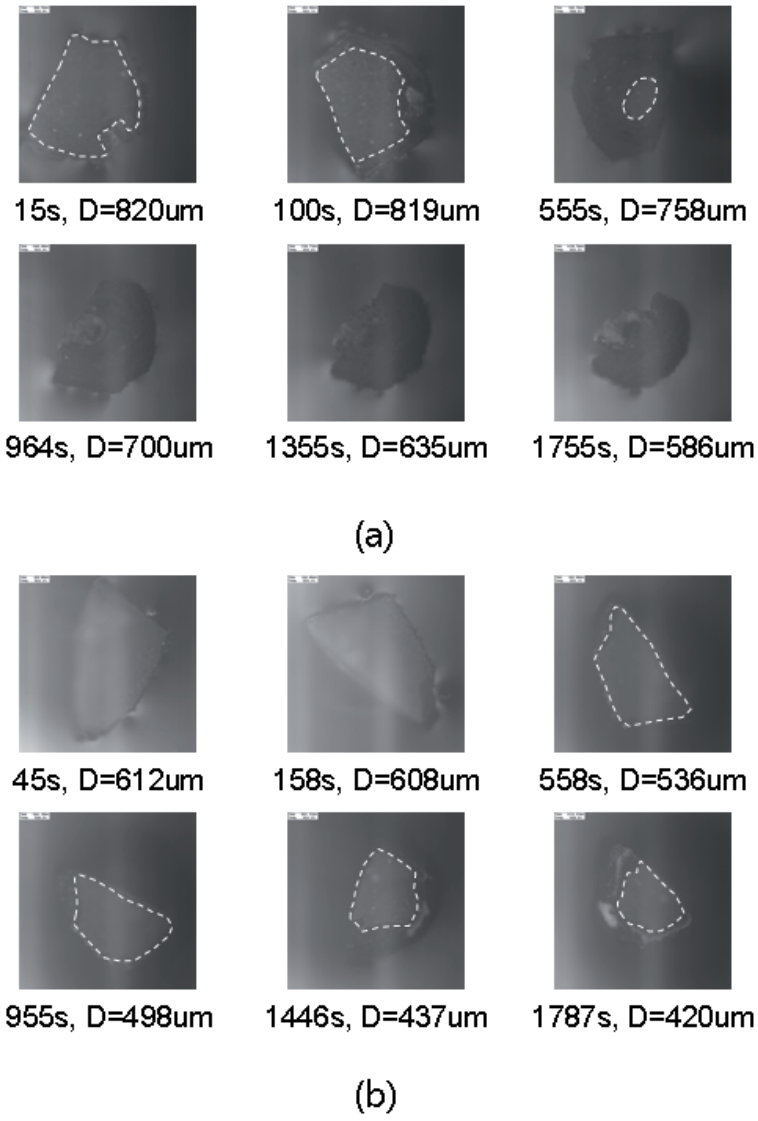

Figure 12: Dissolution sequence of SiC particle in (a) CaO-SiO_2-10 mass% MnO (C/S = 1.0) and (b) CaO-SiO_2-20 mass% MnO (C/S = 0.5) slags at 1873 K under a purified Ar atmosphere (Unwetted area is the inner part of the dashed line).

Hence, the gas evolution will be significant in the composition of high activity of MnO and low activity of SiO_2 at a fixed temperature. This was experimentally confirmed in this study. The evolution of gas bubbles was observed in slag A as shown in Figure 13. One can find small craters indicating the evolution of fine bubbles on the surface of SiC particle wetted by molten slag as shown in Figure 14. Furthermore, the upper portion in Figure 13 seems to get loose from main body due to bubble bursting. Here, the value $p_{Mn}^3 \cdot p_{CO} (= 1.11 \times 10^{-5})$ of this system (slag A) is about 4 times greater than that ($p_{Mn}^3 \cdot p_{CO} (= 2.75 \times 10^{-6})$) of slag B based on thermodynamic calculation.

The size of SiC particle is shown in Figure 15 as a function of reaction time. It seems that the apparent dissolution rate of the SiC particle into the slag A would be slightly faster than that into the slag B. This tendency can be explained not only from the thermodynamics but also from the kinetics view as follows. First, the thermodynamic driving force for the reaction given in Eq. (10) of slag A is greater than that of slag B as discussed in Figures 13 and 14. Second, the viscosity of slag A is lower than that of slag B as shown in Figure 16, which was reproduced from the work by Ji [22]. Even

though the viscosity was measured at 1773 K, the difference in the viscosity between slags A and B could be extrapolated to 1873 K by assuming Newtonian flow at high temperatures.

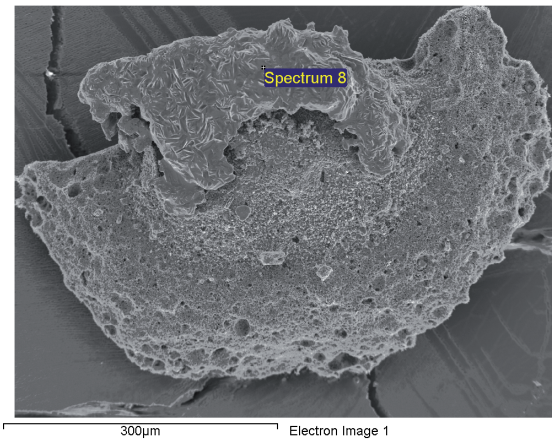

Figure 13: Surface of SiC reacted with CaO-SiO_2-10%MnO (C/S = 1.0) system.

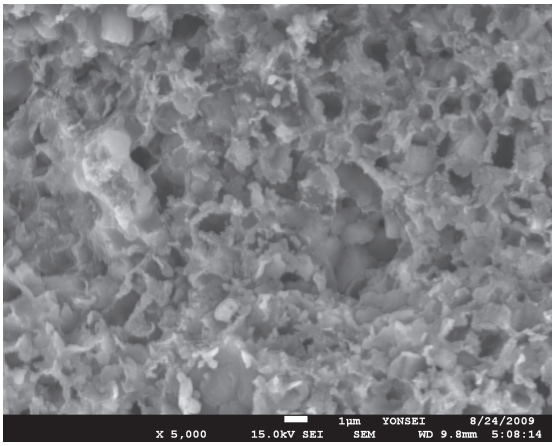

Figure 14: Image of SiC surface magnified from Figure 13.

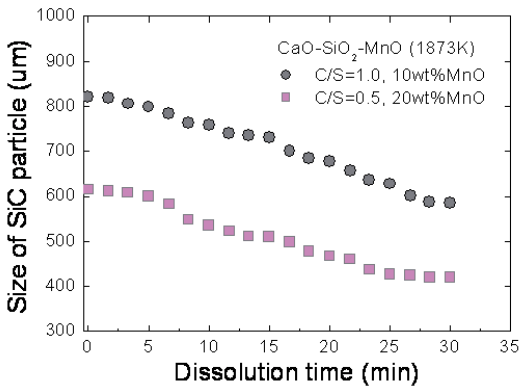

Figure 15: Evolution of the length of SiC particles with time at 1873 K.

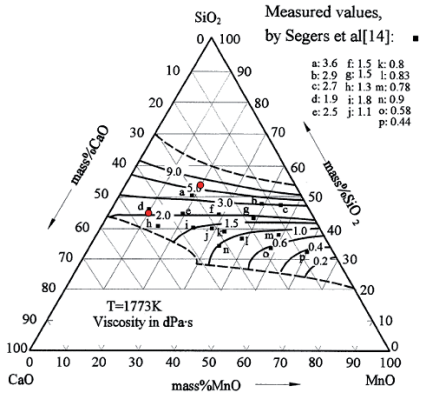

Figure 16: Iso-viscosity of CaO-SiO_2-MnO system at 1773 K. Reproduced from Ref. 22.

However, because the total reaction time was limited to 30 min. at 1873 K in the CSLM experiments, the quantitative analysis for determining the rate-limiting step through the entire dissolution reaction of SiC particle into the slags could not be given in this paper. Thus, the additional CSLM experiments will be carried out in the near future for obtaining the rate-limiting step in a dissolution reaction of SiC particle into the slags at high temperatures.

5 CONCLUSIONS

In the present study, the carbon refining ability of the CaO-SiO_2-MnO slag was measured at 1773 K by employing a carbide capacity concept and thermochemical equilibration methodology. Furthermore, *in-situ* dissolution behaviour of SiC particle into the slag was directly observed by using a confocal scanning laser microscope (CSLM) at 1873 K. The carbide capacity was confirmed to be strongly dependent on the basicity and the stability of carbide ions. In this study, slag basicity was assumed to be in proportion to the activity of lime. The stability of carbide ions was estimated by considering the activity coefficient of CaC_2 in the slag. The carbide capacity also increased with increasing optical basicity of the slag, indicating that the optical basicity can be applied as a measuring index for the carbide capacity of MnO-containing slags. In the CSLM experiments, the SiC particles continuously dissolved into the slag through the wetting phenomena by molten slag and followed by the evolution of gas bubbles. The more basic slags enhanced the wetting of SiC particle by the slag. The fine

bubbles were probably believed to be Mn(g) and CO(g) produced from the reaction between SiC particle and MnO in the slag. The more basic slag also seems to increase the apparent dissolution rate of SiC particles due to lower viscosity. However, the more study should be carried out to reveal the rate-liming step in the dissolution reaction of SiC particle into the slags.

6 REFERENCES

[1] Olsen, S.E., Tangstad, M., Lindstad, T., "Production of Manganese Ferroalloys", SINTEF and Tapir academic press, 2007, pp. 43-110.

[2] Swisher, J.H., Thermodynamics of carbide formation and graphite solubility in the $CaO-SiO_2-Al_2O_3$ system. Trans. TMS-AIME 242 (1968) pp. 2033-2037.

[3] Berryman, R.A., Sommerville, I.D., Carbon solubility as carbide in calcium silicate melts. Metall. Trans. B 23B (1992) 2, pp. 223-227.

[4] Kuwata, M., Suito, H., Solubility of carbon in $CaO-Al_2O_3$ melts. Metall. Mater. Trans. B 27B (1996) 1, pp. 57-64.

[5] Lee, K.R., Suito, H., Solubilities of carbon in $CaO-Al_2O_3-SiO_2$ slags saturated with liquid iron. Steel Res. 67 (1996) 3, pp. 87-92.

[6] Mori, M., Morita, M., Sano, N., Dependence of carbon solubility on oxygen partial pressure for 80 mass% BaO-MnO and $CaO_{satd}-B_2O_3$ slags. Metall. Mater. Trans. B 28B (1997) 6, pp. 1257-1259.

[7] Park, J.H., Min, D.J., Solubility of carbon in $CaO-B_2O_3$ and $BaO-B_2O_3$ slags. Metall. Mater. Trans. B 30B (1999) 6, pp. 1045-1052.

[8] Park, J.H., Min, D.J., Thermodynamic behavior of carbon in molten slags. ISIJ Int. 40 (2000) suppl., pp. S96-S100.

[9] Park, J.H., Min, D.J., Song, H.S., Carbide capacity of $CaO-Al_2O_3-CaF_2$ slag at 1773K. ISIJ Int. 42 (2002) 2, pp. 127-131.

[10] Song, H.S., Kim, D.S., Rhee, C.H., Carbon solubility in steelmaking slag. 2002 Steelmaking Conference Proceeding, ISS-AIME (2002) pp. 301-311.

[11] Park, J.H., Min, D.J., Carbide capacity of $CaO-SiO_2-CaF_2(-Na_2O)$ slags at 1773 K. ISIJ Int. 44 (2004) 2, pp. 223-228.

[12] Watanabe, Y., Kitamura, K., Rachev, I.P., Tsukihashi, F., Sano, N., Thermodynamics of P and S in BaO-MnO flux between 1573 and 1673 K. Metall. Trans. B 24B (1993) 2, pp. 339-347.

[13] Wakasugi, T., Sano, N., Re-evaluation of standard free energy of formation of CaO. Metall. Trans. B 20B (1989) 3, pp. 431-433.

[14] Ono, H., Kobayashi, A., Tsukihashi, F., Sano, N., Determination of standard Gibbs energies of formation of CaC_2, SrC_2 and BaC_2. Metall. Trans. B 23B (1992) 3, pp. 313-316.

[15] Bale, C.W., Chartrand, P., Degterov, S.A., Eriksson, G., Hack, K., Pelton, A.D., Petersen, S., FactSage thermochemical software and databases. Calphad 26 (2002) 2, pp. 189-228.

[16] www.factsage.com.

[17] Turkdogan, E.T., "Physical Chemistry of High Temperature Technology", Academic press, 1980, pp. 1-26.

[18] Liu, J., Verhaeghe, F., Guo, M., Blanpain, B., Wollants, P., "In situ observation of the dissolution of alumina particles in $CaO-Al_2O_3-SiO_2$ melts. J. Am. Ceram. Soc. 90 (2007) 12, pp. 3818-3824.

[19] Duffy, J.A., Optical basicity: A practical acid-base theory for oxides and oxyanions. J. Chem. Edu. 73 (1996) 12, pp. 1138-1142.

[20] Sosinsky, D.J., Sommerville, I.D., The composition and temperature dependence of the sulphide capacity of metallurgical slags. Metall. Trans. B 17B (1986) 3, pp. 331-337.

[21] Safarian, J., Tangstad, M., Wettability of silicon carbide by $CaO-SiO_2$ slags. Metall. Mater. Trans. B. Published online; 01 September 2009.

[22] Ji, F.Z., Experimental studies of the viscosities in $CaO-MnO-SiO_2$ and $CaO-Fe_nO-MnO-SiO_2$ slags. Metall. Mater. Trans. B 32B (2001) 1, pp. 181-186.